Inorg. Chem. **2006**, *45*, 7182–7190

Chemistry of HIV-1 Virucidal Pt Complexes Having Neglected Bidentate sp^2 N-Donor Carrier Ligands with Linked Triazine and Pyridine Rings. Synthesis, NMR Spectral Features, Structure, and Reaction with Guanosine

Vidhi Maheshwari, Debadeep Bhattacharyya, Frank R. Fronczek, Patricia A. Marzilli, and Luigi G. Marzilli*

Department of Chemistry, Louisiana State University, Baton Rouge, Louisiana 70803

Received April 10, 2006

Complexes of the types **L**$PtCl_2$ and $[\mathbf{L}_2Pt]X_2$ [**L** = substituted 3-(pyridin-2′-yl)-1,2,4-triazine] were synthesized and characterized by NMR spectroscopy and, for the first time, by X-ray crystallography in an effort to determine the coordination properties of this novel class of inorganic medicinal agents possessing HIV-1 virucidal activity. The agents containing either one or two sp^2 N-donor bidentate ligands are referred to as **ptt** (platinum triazine) agents. The X-ray structures of three **L**$PtCl_2$ compounds revealed the expected pseudo-square-planar geometry. The X-ray structure of $[(\mathbf{pyPh_2t})_2Pt](BF_4)_2$ [**pyPh$_2$t** = 3-(pyridin-2′-yl)-5,6-diphenyl-1,2,4-triazine] has the expected trans relationship of the unsymmetrical **L** and is essentially planar, an unusual property for a Pt^{II} complex with two bidentate sp^2 N donors. HIV-1 is an RNA virus; the guanosine ribonucleoside (Guo) binds (**MepyMe$_2$t**)$PtCl_2$ at both (inequivalent) available coordination sites to form $[(\mathbf{MepyMe_2t})Pt(Guo)_2]^{2+}$ [**MepyMe$_2$t** = 3-(4′-methylpyridin-2′-yl)-5,6-dimethyl-1,2,4-triazine]. This adduct has four nearly equally intense Guo H8 signals attributed to two pairs of head-to-tail (HT) and head-to-head (HH) conformers, which interchange rapidly within each pair. However, equilibration between pairs requires rotation of the Guo cis to the **MepyMe$_2$t** pyridyl ring, and the H6′ proton on this ring projects toward the Guo and hinders Guo rotation about the Pt–N7 bond. Thus, the HT/HH pairs do not interchange; such behavior is rare. Guo did not add to $[(\mathbf{MepyMe_2t})_2Pt]^{2+}$, a result suggesting the possibility that the virucidal activity of **L**$PtCl_2$ and $[\mathbf{L}_2Pt]^{2+}$ **ptt** agents arises respectively from covalent and noncovalent (possibly intercalative interactions favored by $[\mathbf{L}_2Pt]^{2+}$ planarity) binding to biomolecular targets.

Introduction

In comparison to agents of purely organic molecules, considerably less effort has been devoted to studying metal-containing drugs. Pt complexes, which have been found to be the most promising,[1−7] have the advantages of inertness, low coordination number, and preferential binding to the more limited soft centers in proteins and nucleic acids. The nonleaving carrier ligand on Pt can modify binding sites and thus the activity. Cisplatin [*cis*-$Pt(NH_3)_2Cl_2$] and its analogues, *cis*-PtA_2X_2 (A_2 = two amines or a diamine), interact with DNA by forming a 1,2-intrastrand N7−Pt−N7 cross-link between two adjacent guanines.[8] Pt^{II} compounds also have an extensive history of exhibiting antiviral activity against numerous viruses, including topical antiviral activity.[9−15] In addition, we have clear evidence that the carrier ligand influences the antiviral activity.[13] Structural

* To whom correspondence should be addressed. E-mail: lmarzil@lsu.edu.

(1) Wang, D.; Lippard, S. J. *Nat. Rev. Drug Discovery* **2005**, *4*, 307−320.
(2) Lippert, B., Ed. *Cisplatin: Chemistry and Biochemistry of a Leading Anticancer Drug*; Wiley-VCH: Weinheim, Germany, 1999.
(3) Beljanski, V.; Villanueva, J. M.; Doetsch, P. W.; Natile, G.; Marzilli, L. G. *J. Am. Chem. Soc.* **2005**, *127*, 15833−15842.
(4) Harris, A. L.; Ryan, J. J.; Farrell, N. *Mol. Pharmacol.* **2006**, *69*, 666−672.
(5) van Zutphen, S.; Reedijk, J. *Coord. Chem. Rev.* **2005**, *249*, 2845−2853.
(6) Coluccia, M.; Boccarelli, A.; Mariggió, M.; Cardellicchio, N.; Caputo, P.; Intini, F. P.; Natile, G. *Chem. Biol. Interact.* **1995**, *98*, 251−266.
(7) Quiroga, A. G.; Perez, J. M.; Alonso, C.; Navarro-Ranninger, C.; Farrell, N. *J. Med. Chem.* **2006**, *49*, 224−231.
(8) Blommaert, F. A.; Van Dijk-Knijnenburg, H. C. M.; Dijt, F. J.; Den Engelse, L.; Baan, R. A.; Berends, F.; Fichtinger-Schepman, A. M. J. *Biochemistry* **1995**, *34*, 8474−8480.
(9) Farrell, N.; Bierbach, U. PCT International Application, 1999; p 20.
(10) Sartori, D. A.; Miller, B.; Bierbach, U.; Farrell, N. *J. Biol. Inorg. Chem.* **2000**, *5*, 575−583.

10.1021/ic060605h CCC: $33.50
Published on Web 08/03/2006

Scheme 1. Synthesis of 3-(Pyridin-2′-yl)-5,6-disubstituted-1,2,4-triazine (**L**)

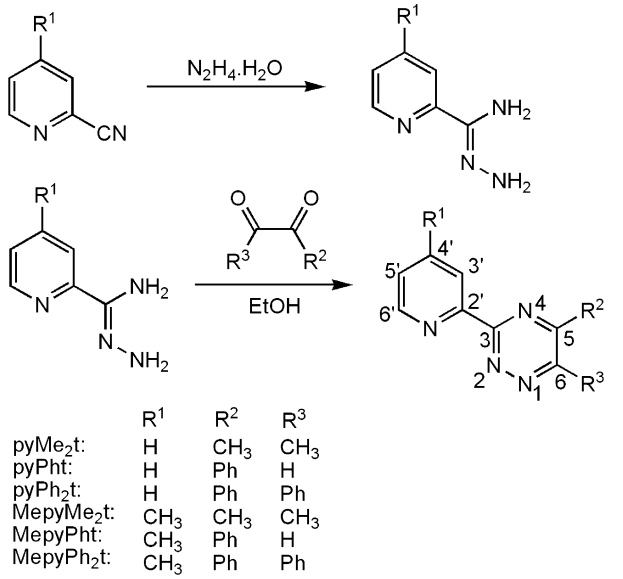

modifications of the carrier ligand in cisplatin may broaden the range of antitumor and antiviral activity and may provide valuable insight into the mechanism of action of the drug.[3,16]

The development of multipurpose drugs with wider application is desirable. Numerous Pt coordination compounds have been synthesized and shown to have both antiviral and antitumor activities.[14] Hybrid drugs of the type *cis*-$[Pt(NH_3)_2(B)Cl]^+$, containing a cisplatin-like moiety and an antiviral Guo-type ligand (B = acyclovir or penciclovir),[14,15] are known. Collaborative studies from this laboratory have shown that Pt compounds containing one or two N-donor aromatic 3-(pyridin-2′-yl)-1,2,4-triazine ligands (**ptt**) possess great potential as anti-HIV microbicides.[13]

The $[(\mathbf{ferene})PtCl_2]^{2-}$ and $[(\mathbf{ferene})_2Pt]^{2-}$ [**ferene** = 3-(pyridin-2′-yl)-5,6-bis(5-sulfo-2-furyl)-1,2,4-triazine; in Scheme 1, $R^2 = R^3 =$ 5-sulfo-2-furyl] complexes are among the most virucidal **ptt** compounds.[13] However, these agents with sulfonated ring substituents were not isolated as crystals, have very complicated ^{1}H NMR spectra, and thus were not well-defined chemically. For example, the triazine ring binding mode (N*2* or N*4*, Scheme 1), or a mixture of such binding modes, could not be resolved for the **ferene** agents.

In this study, we utilize six ligands, **L**, bearing a 3-(pyridin-2′-yl)-1,2,4-triazine moiety (Scheme 1). Three ligands contain the pyridin-2′-yl group: 3-(pyridin-2′-yl)-5,6-dimethyl-1,2,4-triazine (**pyMe$_2$t**), 3-(pyridin-2′-yl)-5-phenyl-1,2,4-triazine (**pyPht**), and 3-(pyridin-2′-yl)-5,6-diphenyl-1,2,4-triazine (**pyPh$_2$t**)). The other three ligands contain the 4′-methylpyridin-2′-yl group: 3-(4′-methylpyridin-2′-yl)-5,6-dimethyl-1,2,4-triazine (**MepyMe$_2$t**), 3-(4′-methylpyridin-2′-yl)-5-phenyl-1,2,4-triazine (**MepyPht**), and 3-(4′-methylpyridin-2′-yl)-5,6-diphenyl-1,2,4-triazine (**MepyPh$_2$t**). We describe here the synthesis of $\mathbf{L}PtCl_2$ and $[\mathbf{L}_2Pt]X_2$ complexes (Scheme 2), along with their characterization by ^{1}H NMR spectroscopy and, for selected examples, by single-crystal X-ray diffraction methods. The pyridyltriazines are relatively neglected ligands; no crystal structures involving 3-(pyridin-2′-yl)-1,2,4-triazines with Pt have been reported. However, crystal structures of **pyPh$_2$t** complexes of Cu,[17] Sn,[18] and Ru[19] have been reported. Also known is a crystal structure of the $[Ce(\mathbf{Mebtp})_3]^{3+}$ [**Mebtp** = 2,6-bis(5,6-dimethyl-1,2,4-triazin-3-yl)-pyridine] complex with the **Mebtp** tridentate ligand containing the **pyMe$_2$t** moiety.[20]

Scheme 2. Synthesis of $\mathbf{L}PtCl_2$ and $[\mathbf{L}_2Pt]^{2+}$ Complexes[a]

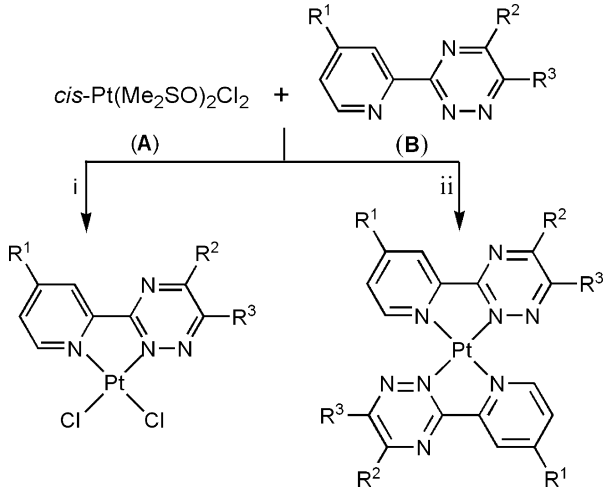

[a] Reagents and conditions: (i) A:B = 1:1, CH_3OH, 60 °C, 12 h; (ii) A:B = 1:2, CH_3OH, 60 °C, 24 h.

Pt^{II} compounds have a high affinity for reacting with S-containing biomolecules such as methionine and also with N7 of purine bases in nucleic acids, but the target for virucidal activity is not known. Carrier-ligand bulk plays a role in influencing both biological activity and the properties of adducts. Because Pt complexes of 3-(pyridin-2′-yl)-1,2,4-triazines may form 1,2-intrastrand GG cross-links with RNA in HIV-1 and because the observation of rotamers formed by restricted rotation about the N7 bonds in $Pt(Guo)_2$ adducts provides information on ligand steric bulk, we assessed whether rotamers can be detected for $[(\mathbf{MepyMe_2t})Pt(Guo)_2]^{2+}$. The carrier ligands in cisplatin and other Pt^{II} anticancer drugs usually are not bulky enough to impede the rotation of N7-bound guanine about the Pt−N7 bond, but planar sp^2 N-donor ligands such as 5,5′-dimethyl-2,2′-

(11) Snyder, M. B.; Saravolatz, L. D.; Markowitz, N.; Pohlod, D.; Taylor, R. C.; Ward, S. G. *J. Antimicrob. Chemother.* **1987**, *19*, 815−822.
(12) Taylor, R. C.; Ward, S. G.; Schmidt, P. P. U.S. Patent Application, 1986; p 4.
(13) Vzorov, A. N.; Bhattacharyya, D.; Marzilli, L. G.; Compans, R. W. *Antiviral Res.* **2005**, *65*, 57−67.
(14) Balcarová, Z.; Kašpárková, J.; Žákovská, A.; Novakává, O.; Sivo, M. F.; Natile, G.; Brabec, V. *Mol. Pharmacol.* **1998**, *53*, 846−855.
(15) Margiotta, N.; Bergamo, A.; Sava, G.; Padovano, G.; De Clercq, E.; Natile, G. *J. Inorg. Biochem.* **2004**, *98*, 1385−1390.
(16) Fuertes, M. A.; Alonso, C.; Perez, J. M. *Chem. Rev.* **2003**, *103*, 645−662.
(17) Uma, R.; Palaniandavar, M.; Butcher, R. J. *J. Chem. Soc., Dalton Trans.* **1996**, *10*, 2061−2066.
(18) Prasad, L.; Page, L. E.; Smith, F. E. *Inorg. Chim. Acta* **1983**, *68*, 45−49.
(19) Pal, P. K.; Chowdhury, S.; Drew, M. G. B.; Datta, D. *New J. Chem.* **2000**, *24*, 931−933.
(20) Iveson, P. B.; Riviere, C.; Guillaneux, D.; Nierlich, M.; Thuery, P.; Ephritikhine, M.; Madic, C. *J. Chem. Soc., Chem. Commun.* **2001**, 1512−1513.

bipyridine (**5,5′-Me$_2$bipy**)[21] and 1,10-phenanthroline (**phen**)[22] allow the detection of rotamers on the NMR time scale. The aromatic portion of the 3-(pyridin-2′-yl)-1,2,4-triazine carrier ligands in **ptt** compounds can also possibly intercalate into nucleic acids.[23] Thus, all of these reasons prompted us to conduct this study of the synthesis and characterization of **ptt** compounds related to **ptt** compounds with **ferene** that are known to be HIV-1 virucidal.[13]

Experimental Section

Starting Materials. The starting material, pyridine-2-carboxamide hydrazone (2-pyridylamidrazone), was synthesized by a known method[24] (Scheme 1) in yields above 90%. 4′-Methyl-substituted pyridine-2-carboxamide hydrazone (4′-methyl-2-pyridylamidrazone) was synthesized as described by Case.[25] Guanosine (Guo; Sigma) and **pyPh$_2$t** (Fluka) were obtained from commercial sources. *cis*-Pt(Me$_2$SO)$_2$Cl$_2$ was prepared as described in the literature.[26] Elemental analyses (C, H, and N) were performed by Atlantic Microlabs, Atlanta, GA.

NMR Measurements. ^{1}H NMR spectra were recorded on Bruker spectrometers operating at 400 or 500 MHz. We used the values of 0.00 and 4.78 ppm to reference signals to tetramethylsilane in deuterated dimethyl sulfoxide (DMSO-d_6) solutions and to the residual HOD signal in deuterated water (D$_2$O)/DMSO-d_6 solutions, respectively. DNO$_3$ and NaOD solutions (0.1 M in D$_2$O) were used to adjust the pH of D$_2$O/DMSO-d_6 solutions. 2D ROESY experiments[27] were performed at 25 °C by using a 500-ms mixing time (128 scans per t_1 increment). NMR data were processed with XWINNMR or Mestre-C software.

Synthesis of L = 3-(Pyridin-2′-yl)-5,6-disubstituted-1,2,4-triazine and 3-(4′-Methylpyridin-2′-yl)-5,6-disubstituted-1,2,4-triazine. The **pyMe$_2$t**, **pyPht**, and **pyPh$_2$t** ligands and their 3-(4-methylpyridin-2′-yl) analogues, **MepyMe$_2$t**, **MepyPht**, and **MepyPh$_2$t**, were prepared as described in the literature[25,28,29] (Scheme 1), with minor modifications. An ethanol solution (30 mL) containing 2-pyridylamidrazone, or its 4′-methyl analogue (2.5 mmol), and an α-diketone (2.5 mmol) was heated at reflux for 3 h. The volume of the solution was reduced to one-fourth by rotary evaporation. The addition of an excess of hexane afforded the desired pure crystalline 3-(pyridin-2′-yl)-1,2,4-triazine in 90% yield.

Synthesis of LPtCl$_2$ Complexes. Two methods, A and B, were employed to obtain **L**PtCl$_2$ complexes (Scheme 2). Method A involved heating of a methanol solution (30 mL) of *cis*-Pt(Me$_2$SO)$_2$Cl$_2$ (0.101 g, 0.24 mmol) and **L** (0.24 mmol) at 60 °C for 12 h. The yellow solid that precipitated was collected, washed with diethyl ether followed by chloroform, and dried in vacuo. Method A resulted in high yields of a powdered **L**PtCl$_2$ product that required no further purification. Method B, employed to obtain X-ray-quality crystals, involved mixing of an acetonitrile solution of *cis*-Pt(Me$_2$SO)$_2$Cl$_2$ (4.22 mg,10 mM in 1 mL) with **L** (10 mM in 1 mL) and allowing this mixture to stand at 23 °C. Thin needles of **L**PtCl$_2$, varying in color from greenish-yellow to orange, were obtained in ∼15% yield after 24 h.

(pyMe$_2$t)PtCl$_2$ (1). Method A gave a yellow precipitate: yield = 0.077 g (71%). Method B afforded orange needle-shaped crystals. ^{1}H NMR (ppm) in DMSO-d_6: 9.57 (d, H6′), 8.60 (d, H3′), 8.48 (t, H4′), 8.03 (t, H5′), 2.75 (s, CH$_3$), 2.59 (s, CH$_3$). Anal. Calcd for C$_{10}$H$_{10}$Cl$_2$N$_4$Pt: C, 26.56; H, 2.23; N, 12.39. Found: C, 26.77; H, 2.29; N, 12.37.

(pyPht)PtCl$_2$ (2). Method A gave a yellow powder: yield = 0.084 g (75%). Method B produced yellow-green needles. ^{1}H NMR (ppm) in DMSO-d_6: 10.18 (s, H6), 9.62 (d, H6′), 8.78 (d, H3′), 8.54 (t, H4′), 8.11 (t, H5′), 8.64 (d, *o*-PhH), 7.85 (t, *p*-PhH), 7.71 (t, *m*-PhH). Anal. Calcd for C$_{14}$H$_{10}$Cl$_2$N$_4$Pt: C, 33.61; H, 2.01; N, 11.20. Found: C, 33.48; H, 1.95; N, 11.10.

(pyPh$_2$t)PtCl$_2$ (3). Method A gave a yellow solid: yield = 0.099 g (83%). Orange needles were obtained by method B. ^{1}H NMR (ppm) in DMSO-d_6: 9.63 (d, H6′), 8.62 (d, H3′), 8.53 (t, H4′), 8.09 (t, H5′), 7.38−7.51 (PhH). Anal. Calcd for C$_{20}$H$_{14}$Cl$_2$N$_4$Pt: C, 41.68; H, 2.45; N, 9.72. Found: C, 41.45; H, 2.37; N, 9.80.

(MepyMe$_2$t)PtCl$_2$ (4). Method A resulted in a yellow powder: yield = 0.096 g (77%). X-ray-quality crystals in the form of yellow needles were obtained by method B. ^{1}H NMR (ppm) DMSO-d_6: 9.35 (d, H6′), 8.26 (s, H3′), 7.85 (d, H5′), 2.74 (s, CH$_3$), 2.57 (s, CH$_3$), 2.53 (s, CH$_3$). Anal. Calcd for C$_{11}$H$_{12}$Cl$_2$N$_4$Pt: C, 28.34; H, 2.59; N, 12.02. Found: C, 28.32; H, 2.58; N, 11.82.

(MepyPht)PtCl$_2$ (5). The complex was obtained as a yellow powder by method A: yield = 0.095 g (68%). ^{1}H NMR (ppm) in DMSO-d_6: 10.15 (s, H6), 9.41 (d, H6′), 8.61 (s, H3′), 7.91 (d, H5′), 8.65 (d, *o*-PhH), 7.84 (t, *p*-PhH), 7.70 (t, *m*-PhH), 2.59 (s, CH$_3$). Anal. Calcd for C$_{15}$H$_{12}$Cl$_2$N$_4$Pt: C, 35.03; H, 2.35; N, 10.89. Found: C, 34.81; H, 2.31; N, 10.65.

(MepyPh$_2$t)PtCl$_2$ (6). Method A resulted in a reddish-yellow precipitate: yield = 0.112 g (79%). Method B produced yellow needles. ^{1}H NMR (ppm) in DMSO-d_6: 9.44 (d, H6′), 8.49 (s, H3′), 7.93 (d, H5′), 7.75 (d, *o*-PhH), 7.45−7.63 (*m*, *p*-PhH), 2.58 (s, CH$_3$). Anal. Calcd for C$_{21}$H$_{16}$Cl$_2$N$_4$Pt: C, 42.72; H, 2.73; N, 9.49. Found: C, 42.75, H, 2.58; N, 9.43.

Synthesis of [L$_2$Pt]X$_2$ Salts. *cis*-Pt(Me$_2$SO)$_2$Cl$_2$ (0.042 g, 0.1 mmol) was added to a methanol solution of **L** (0.4 mmol, 10 mL), and the resulting suspension became a solution when stirred at 60 °C for 24 h (Scheme 2). The mixture was allowed to cool to room temperature. Any precipitate that formed was removed by filtration, and the clear filtrate was treated with a methanol solution of an excess of NaBF$_4$ or NaPF$_6$ to precipitate the [**L**$_2$Pt]X$_2$ salt. The solid was collected, washed twice with methanol followed by anhydrous diethyl ether, and allowed to dry in air. Yields of the [**L**$_2$Pt]X$_2$ salts were 35−45%. The ^{1}H NMR spectra and shifts for representative [**L**$_2$Pt]X$_2$ complexes appear in the Supporting Information.

[(pyPht)$_2$Pt](PF$_6$)$_2$ (7). The method described above afforded a yellow solid upon the addition of an excess of NaPF$_6$: yield = 0.30 g (36%). The ^{1}H NMR spectra of the BF$_4$ and PF$_6$ salts were identical. Anal. Calcd for C$_{28}$H$_{20}$N$_8$P$_2$F$_{12}$Pt: C, 35.27; H, 2.11; N, 11.75. Found: C, 35.54; H, 1.89; N, 11.85.

[(pyPh$_2$t)$_2$Pt](BF$_4$)$_2$ (8). Crystals were obtained by the general method described above, but by very careful dropwise addition of a methanol solution of NaBF$_4$ (5 mmol) to the filtrate until the solution first became cloudy. Thin, yellow, needle-shaped crystals were obtained by allowing the solution to stand undisturbed for 2 days.

(21) Bhattacharyya, D.; Marzilli, P. A.; Marzilli, L. G. *Inorg. Chem.* **2005**, *44*, 7644−7651.
(22) Margiotta, N.; Papadia, P.; Fanizzi, F. P.; Natile, G. *Eur. J. Inorg. Chem.* **2003**, 1136−1144.
(23) Collins, J. G.; Rixon, R. M.; Wright, J. R. A. *Inorg. Chem.* **2000**, *39*, 4377−4379.
(24) Hage, R.; Van Diemen, J. H.; Ehrlich, G.; Haasnoot, J. G.; Stufkens, D. J.; Snoeck, T. L.; Vos, J. G.; Reedijk, J. *Inorg. Chem.* **1990**, *29*, 988−993.
(25) Case, F. H. *J. Org. Chem.* **1965**, *30*, 931−933.
(26) Price, J. H.; Williamson, A. N.; Schramm, R. F.; Wayland, B. B. *Inorg. Chem.* **1972**, *11*, 1280−1284.
(27) Sullivan, S. T.; Ciccarese, A.; Fanizzi, F. P.; Marzilli, L. G. *J. Am. Chem. Soc.* **2001**, *123*, 9345−9355.
(28) Hage, R.; Haasnoot, J. G.; Reedijk, J. *Inorg. Chim. Acta* **1990**, *172*, 19−23.
(29) Islam, M. A.; Stephen, W. I. *Talanta* **1992**, *39*, 1429−1435.

Table 1. Crystal Data and Structure Refinement for **L**$PtCl_2$ [**L** = **pyMe$_2$t** (**1**), **pyPht** (**2**), **pyPh$_2$t** (**3**)] and [(**pyPh$_2$t**)$_2$Pt]$(BF_4)_2$ (**8**)

	1	**2**	**3**	**8**
empirical formula	$C_{10}H_{10}Cl_2N_4Pt$	$C_{14}H_{10}Cl_2N_4Pt$	$C_{20}H_{14}Cl_2N_4Pt{\cdot}CH_3CN$	$C_{40}H_{28}B_2F_8N_8Pt\cdot 0.59H_2O$
fw	452.21	500.25	617.40	1000.00
space group	*Pbca*	$P2_1/c$	$P2_1/c$	$C2/c$
unit cell dimens				
a (Å)	7.3055(10)	9.236(5)	10.202(2)	35.253(5)
b (Å)	17.923(4)	7.496(4)	7.4820(10)	7.8417(15)
c (Å)	17.977(4)	19.789(13)	27.278(7)	13.811(3)
β (deg)	90	94.312(18)	93.513(7)	99.270(7)
V (Å^3)	2353.8(8)	1366.2(14)	2078.3(7)	3768.1(12)
T (K)	102	100	100	110
Z	8	4	4	4
ρ_{calc} (mg/m^3)	2.552	2.432	1.973	1.763
abs coeff (mm^{-1})	12.356	10.658	7.029	3.809
$2\theta_{max}$ (deg)	65.2	55.0	63.0	56.6
R1 indices[a]	0.029	0.062	0.034	0.033
wR2 [$I > 2\sigma(I)$][b]	0.060	0.155	0.059	0.065
data/param	4267/157	3085/190	6483/272	4639/275

[a] $R1 = (\sum||F_o| - |F_c||)/\sum|F_o|$. [b] $wR2 = [\sum[w(F_o^2 - F_c^2)^2]/\sum[w(F_o^2)^2]]^{1/2}$, in which $w = 1/[\sigma^2(F_o^2) + (0.0787P)^2]$ and $P = (F_o^2 + 2F_c^2)/3$.

[(MepyPh$_2$t)$_2$Pt](PF$_6$)$_2$ (9). This product was obtained as a yellow solid in the same way as **7** was; yield = 0.041 g (40%). The ^{1}H NMR spectra of the BF_4 and PF_6 salts were identical. Anal. Calcd for $C_{42}H_{32}N_8P_2F_{12}Pt$: C, 44.49; H, 2.84; N, 9.88. Found: C, 44.58; H, 2.68; N, 9.94.

Reaction of ptt's with Guo. A 14 mM (1.63 mg) solution of (**MepyMe$_2$t**)$PtCl_2$ (**4**) in DMSO-d_6 (250 μL) was treated with a Guo solution (1.98 mg, 15.5 mM in 450 μL of D_2O) to give a 1:2 ratio (5 mM to 10 mM ratio) of Pt/Guo, and the solution (pH ~4.6) was kept at 25 °C. The mixture of D_2O and DMSO-d_6 solutions was used to improve the solubility of **4**. The pH of the solution decreased with time and had to be adjusted to ~4.6. The solution was monitored for 6 days until the ^{1}H NMR signals of free Guo disappeared. However, the reaction was repeated several times, and to decrease the time for the reaction to reach completion, an excess of Guo was often employed. A DMSO-d_6 solution (250 μL) of [(**MepyMe$_2$t**)$_2$Pt]$(BF_4)_2$ (2.69 mg, 14 mM) was treated with a Guo (1.98 mg, 15.5 mM) solution in D_2O (450 μL) to give a 1:2 ratio of Pt/Guo, and the solution was maintained at pH ~4.6 at 25 °C. The solution was monitored by ^{1}H NMR spectroscopy, and no evidence of any reaction was found even after 36 h.

X-ray Data Collection and Structure Determination. Single crystals were placed in a cooled N_2 gas stream at ~100 K on a Nonius Kappa CCD diffractometer fitted with an Oxford Cryostream cooler with graphite-monochromated Mo Kα (0.710 73 Å) radiation. Data reduction included absorption corrections by the multiscan method, with HKL SCALEPACK.[30]

All X-ray structures were determined by direct methods and difference Fourier techniques and refined by full-matrix least squares, using *SHELXL97*.[31] All non-H atoms were refined anisotropically. All H atoms were visible in difference maps but were placed in idealized positions. A torsional parameter was refined for each methyl group. For all structures, the maximum residual densities were located near the Pt positions.

Results and Discussion

X-ray Crystallography. Structures of pseudo-square-planar complexes reported here include **L**$PtCl_2$ (**L** = **pyMe$_2$t**, **pyPht**, and **pyPh$_2$t**) and [(**pyPh$_2$t**)$_2$Pt]$(BF_4)_2$ (**8**) (Tables 1 and2 and Figures 1 and 2). The atom-numbering systems in these ORTEP figures are used to discuss only these solid-state data. A superscript i denotes the atoms of the other ligand in **8**. For all other references to pyridyltriazine ligands and complexes (e.g., NMR discussion), the atom numbering in Scheme 1 will be used, and in the text, the number will be in italics. In some cases, we shall designate the Pt-bound N's as N(t) and N(py), in the triazine and pyridine rings, respectively. The numbering scheme for bipyridines is given in Figure 3 and for guanosine in Figure 8.

Table 2. Selected Bond Distances (Å) and Angles (deg) for **L**$PtCl_2$ [**L** = **pyMe$_2$t** (**1**), **pyPht** (**2**), **pyPh$_2$t** (**3**)] and [(**pyPh$_2$t**)$_2$Pt]$(BF_4)_2$ (**8**)

	1	**2**	**3**	**8**
		Bond Distances		
Pt−N1	2.001(3)	1.996(11)	1.996(3)	2.019(3)
Pt−N4	2.020(3)	2.011(11)	2.027(3)	2.050(3)
Pt−Cl1	2.2969(11)	2.304(4)	2.2920(10)	Pt−N4^i 2.050(3)
Pt−Cl2	2.2899(10)	2.292(4)	2.2972(10)	Pt−N1^i 2.019(3)
		Bond Angles		
N4−Pt−N1	80.33(12)	79.8(4)	80.38(11)	78.68(13)
N1−Pt−Cl1	174.83(9)	173.3(3)	174.90(8)	N1−Pt−N1^i 180.0
N1−Pt−Cl2	96.05(9)	96.2(3)	95.86(8)	N1−Pt−N4^i 101.32(13)
N4−Pt−Cl1	94.50(10)	93.8(3)	94.60(8)	N4−Pt−N1^i 101.32(13)
N4−Pt−Cl2	176.30(9)	176.0(3)	176.24(8)	N4−Pt−N4^i 180.0
Cl2−Pt−Cl1	89.13(3)	90.12(13)	89.16(3)	N4^i−Pt−N1^i 78.68(13)
C5−C4−C3	123.0(3)	124.7(13)	122.9(3)	123.1(4)
N4−C4−C3	114.1(3)	113.6(12)	114.5(3)	114.4(3)
N3−C3−C4	120.1(3)	119.4(12)	121.0(3)	120.6(3)
N1−C3−C4	114.8(3)	114.2(11)	115.0(3)	114.6(3)

To discuss structural features of the pyridyltriazine ligands, we shall use some of the terminology employed for the common symmetrical sp^2 N-donor **L**'s, e.g., 2,2′-bipyridine (**bipy**) or **phen** ligands. The M−N distance for which there would be no in-plane distortion (Figure 3) has been estimated to be 2.72 Å.[32] Hazell and co-workers concluded that the stress in coordinated **bipy**'s caused by the close proximity of the H atoms on the C atoms ortho to the bridging atoms is reduced by the twisting of the pyridine rings about the bond bridging the two pyridine rings and by an in-plane bending (Figure 3).[33] Likewise, in compounds such as

(30) Otwinowski, Z.; Minor, W. *Macromolecular Crystallography*; New York Academic Press: New York, 1997; Vol. 276, Part A.
(31) Sheldrick, G. M. *SHELXL97, Program for Crystal Structure Solution and Refinement*; University of Göttingen: Göttingen, Germany, 1997.
(32) Hazell, A. *Polyhedron* **2004**, *23*, 2081−2083.
(33) Hazell, A.; Simenson, O.; Wernberg, O. *Acta Crystallogr*. **1986**, *C42*, 1707−1711.

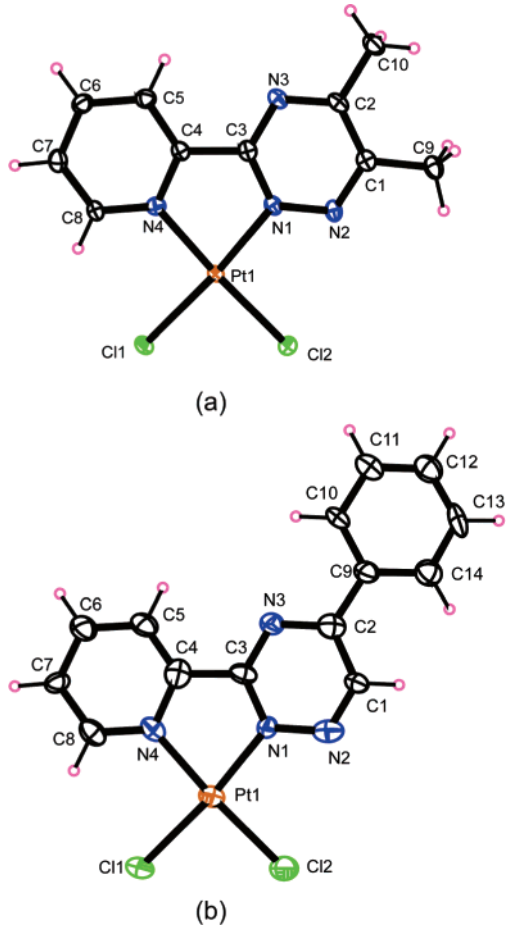

Figure 1. ORTEP plots of (a) (**pyMe$_2$t**)PtCl$_2$ (**1**) and (b) (**pyPht**)PtCl$_2$ (**2**). Thermal ellipsoids are drawn with 50% probability.

[(**bipy**)$_2$Pt]$^{2+}$, the M−N distance for which there would be no distortion of the overall coordination environment from planarity has been estimated to be 2.8 Å.[34] Therefore, we begin our discussion of the structures with bond lengths and angles involving Pt.

Structures of LPtCl$_2$. (a) Coordination Parameters. The size of the group on the C1 and C2 positions has little effect on the coordinated bond distances and angles (Table 2). The Pt−Cl or Pt−N(py) bond distances found for **1**−**3** are not significantly different from those in the structure of (**4,4′-Me$_2$bipy**)PtCl$_2$ (work in progress). All three **L**PtCl$_2$ complexes and (**4,4′-Me$_2$bipy**)PtCl$_2$ have comparable N−Pt−N bite angles. For **1** and **3**, in which the Pt−N distances are more precisely determined, the Pt−N(py) bond (Pt−N4) is slightly longer than the Pt−N(t) bond (Pt−N1) (Table 2). We attribute this apparently slightly smaller Pt−N(t) bond to an attractive interaction of the positive Pt center with the lone pair on N2, the triazine N bound to N1. In contrast, the H on the C8 atom of the pyridine ring (in the position corresponding to N2) will have a repulsive interaction with the positive Pt center.

In **1**−**3**, the *cis*-N(t)−Pt−Cl2 angle is significantly larger than the *cis*-N(py)−Pt−Cl1 angle. There is a slight attractive interaction between Cl's cis to a pyridyl ring and the nearby

(34) Rund, J. V. *Inorg. Chem.* **1967**, *7*, 24−27.

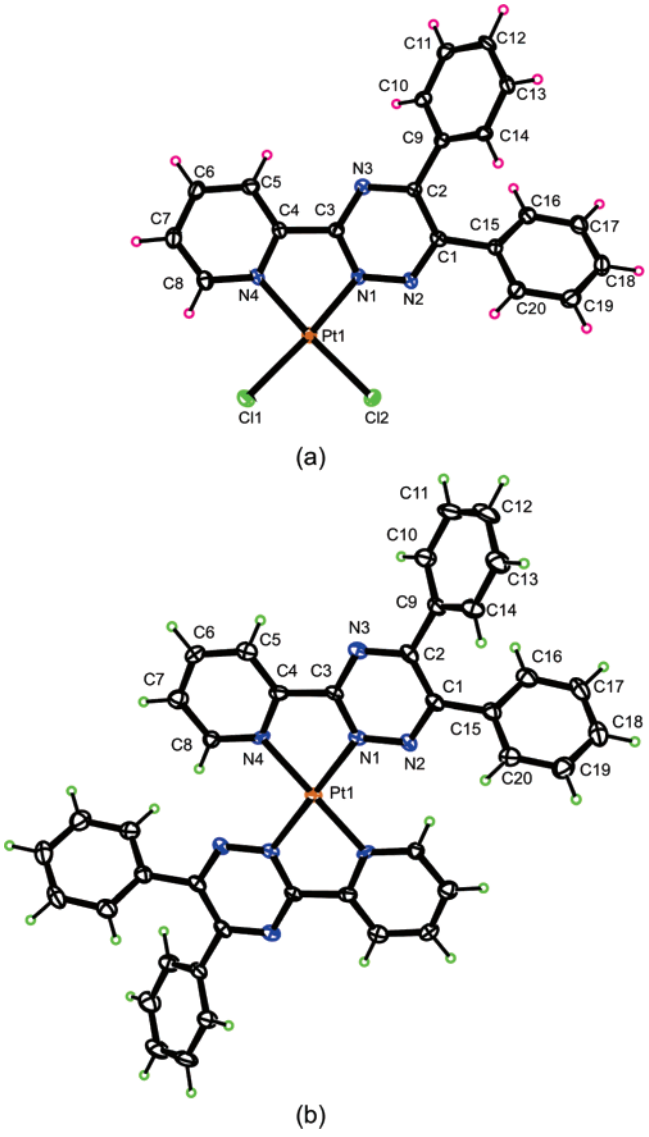

Figure 2. ORTEP plots of (a) (**pyPh$_2$t**)PtCl$_2$ (**3**) and (b) [(**pyPh$_2$t**)$_2$Pt](BF$_4$)$_2$ (**8**). Thermal ellipsoids are drawn with 50% probability.

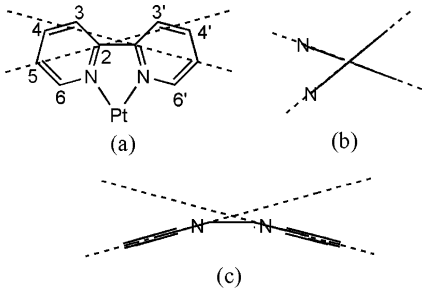

Figure 3. Distortions in bipyridyl ligands: (a) in-plane, (b) twist, and (c) bowing.

pyridine ring H atom (labeled A, Figure 4). The repulsion (labeled R, Figure 4) between the lone pair on N2 and the cis Cl creates a larger than normal N−Pt−Cl angle. The apparent net effects of the nonbonding interactions involving the lone pair are a shorter Pt−N(t) bond and a wider *cis*-N(t)−Pt−Cl angle.

(b) Bidentate Ligand Parameters. Distortions in the ligand (Figure 3) will occur if the M−N distance is typical

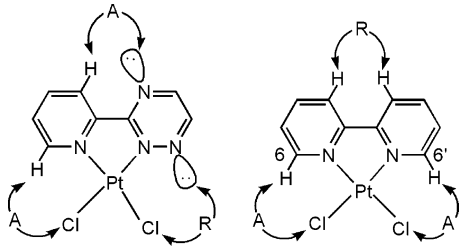

Figure 4. Attractive and repulsive interactions in **L**$PtCl_2$ and (**bipy**)$PtCl_2$.

(∼2.0−2.2 Å).[33] Because the distances of the C*3*H and C*3*′H atoms of bipyridines (Figure 3) to the C*3*′ and H*3*′ atoms and the C*3* and H*3* atoms on the other ring, respectively, are less than the sum of the van der Waals radii,[35] it has been suggested that the resulting repulsive interactions (labeled R, Figure 4) cause distortions.[32,33] The difference in two exocyclic angles (C5−C4−C3 and N4−C4−C3; see Figure 2) of the pyridine ring can be used as a simple means for estimating the in-plane bending (Figure 3).[33] The differences in these two angles for (**4,4′-Me$_2$bipy**)$PtCl_2$ are comparable to the differences for **L**$PtCl_2$ complexes (Table 2), although for **L**$PtCl_2$ complexes, the H on the pyridyl C ortho to the bridging C atoms and the lone-pair-bearing triazine N3 (in **3**, Figure 2, the H5−N3 distance = 2.630 Å and the C5−N3 distance = 2.900 Å) should create a slight favorable attractive interaction (labeled A, Figure 4). Therefore, any stress due to H*3*−H*3*′ repulsion in (**4,4′-Me$_2$bipy**)-$PtCl_2$ does not lead to an apparent substantial effect on the in-plane bending. However, this repulsion could account for the slight twisting or bowing in (**4,4′-Me$_2$bipy**)$PtCl_2$ compared to the minimal distortions found for the three **L**$PtCl_2$ complexes (Figure 5).

Structure of [(pyPh$_2$t)$_2$Pt](BF$_4$)$_2$ (8). (a) Coordination Parameters. The ORTEP drawing for **8** appears in Figure 2. The Pt−N(py) bond length [2.050(3) Å] in **8** is similar to the Pt−N(py) bond length [2.032(3) Å] in [(**4,4′-Me$_2$bipy**)$_2$-Pt](BF$_4$)$_2$ (work in progress), but it is significantly longer than the Pt−N(t) bond distance [2.019(3) Å] in **8** (Table 2). The reason for the shorter Pt−N(t) bond distance was suggested above. The N−Pt−N bite angle in **8** is similar to that in [(**4,4′-Me$_2$bipy**)$_2$Pt](BF$_4$)$_2$. These N−Pt−N bite angles are slightly smaller than those for **L**$PtCl_2$ (Table 2). The Pt−N bond distances in **8** are larger than the corresponding bond distances in **3**.

(b) Relative Bidentate Ligand Relationships. The ligand distortion due to in-plane bending for **8** was less than that for [(**4,4′-Me$_2$bipy**)$_2$Pt](BF$_4$)$_2$ but comparable with those of **L**$PtCl_2$ (Table 2). For bipyridine complexes with ∼2-Å M−N distances, the strain induced by the close approach of the H atoms of opposing ligands can be reduced by two different types of distortions. First, a tetrahedral deformation at the metal can occur, resulting in the ligands being canted relative to each other (Figure 6). Second, the ligand rings can be bowed away from the ring directly across (Figure 6).[32,33,36] The opposing ligands in [(**4,4′-Me$_2$bipy**)$_2$Pt](BF$_4$)$_2$ are bow-like distorted (Figure 7), while canting of the two ligands occurs in [(**2,2′-bipy**)$_2$Pt](NO$_3$)$_2$.[33] In contrast, for **8**, the Pt lies on an inversion center, and the coordination geometry is totally planar and symmetrical (Figure 7). In [(**4,4′-Me$_2$bipy**)$_2$Pt](BF$_4$)$_2$, the distances found between H*6* (H on the C ortho to the N; Figure 3) and the opposing C*6* of the other ligand are 2.557 and 2.597 Å. For **8**, in contrast, the distance between the related pyridyl proton (H8; Figure 2) and the opposing triazine nonbonded N2 of the other ligand is 2.160 Å. The unusually small distance suggests the possibility of two weak favorable H···N interactions between the two opposing **pyPh$_2$t** ligands of **8**. Thus, the metal center exhibits no distortion.

NMR Spectroscopy. As mentioned, both the reaction of **ferene** with *cis*-Pt(Me$_2$SO)$_2$Cl$_2$ and the resulting products are difficult to assess by ^{1}H NMR spectroscopy because of many overlapping signals. Also, simpler 3-(pyridin-2′-yl)-1,2,4-triazines (**L**) analogues, which form **L**$PtCl_2$ and [**L**$_2$-Pt]$^{2+}$ complexes with less complicated spectra, have not been studied. Hence, we have investigated by ^{1}H NMR spectroscopy the formation and properties, such as the degree of solvolysis, of these simpler **ptt** compounds. We use the standard numbering system for these **L**'s (Scheme 1).

Reactions of **L** (20 mM) with *cis*-Pt(Me$_2$SO)$_2$Cl$_2$ (5 mM) in DMSO-d_6 were monitored with time until no further changes were observed. The H*6*′ doublet was usually observed between ∼9.3 and 9.6 ppm within ∼1 h of mixing. After ∼1 day, a weaker doublet appeared farther downfield (∼10.0−10.2 ppm). (These findings are consistent with the **ferene** results: H*6*′ doublet at ∼9.6 ppm for [(**ferene**)$PtCl_2$]$^{2-}$ and at ∼10.7 ppm for [(**ferene**)$_2$Pt]$^{2-}$.[13]) The addition of [NEt$_4$]Cl caused an increase in the intensity of the doublet between 9.3 and 9.6 ppm and the disappearance of the more downfield doublet (∼10−10.2 ppm), indicating that these are signals of **L**$PtCl_2$ and [**L**$_2$Pt]$^{2+}$, respectively.

For all **L**'s, [**L**$_2$Pt]$^{2+}$ did not form completely and was less abundant than **L**$PtCl_2$ in DMSO-d_6, even with a 3-fold excess of **L**. To form bis-product exclusively, D_2O (10 vol %) was added to a separate solution of **L** and *cis*-Pt(Me$_2$SO)$_2$Cl$_2$ (in a 4:1 ratio). After ∼1 h, the [**L**$_2$Pt]$^{2+}$ signals were the only bound **L** signals present. The greater solvation of the Cl^- ions in D_2O compared to that in DMSO-d_6 facilitates the formation of bis-complexes. The reaction of **pyMe$_2$t** with *cis*-Pt(Me$_2$SO)$_2$Cl$_2$ described in the Supporting Information provides a detailed set of results that are representative of studies with other **L**'s.

[(MepyMe$_2$t)Pt(Guo)$_2$]$^{2+}$ Characterization. Within 30 min of mixing **4** and Guo in a 1:2 molar ratio in a D_2O/DMSO-d_6 solution at pH 4.60 at 25 °C, the [(**MepyMe$_2$t**)-Pt(Guo)$_2$]$^{2+}$ adduct was formed. The adduct has H8 signals at ∼8.7−8.9 ppm, downfield from the free Guo H8 signal at 8.11 ppm, indicating that Guo is bound to Pt via N7. Two guanine base arrangements, HH (head-to-head) and HT (head-to-tail), are possible for [**L**Pt(Guo)$_2$]$^{2+}$-type adducts. Three rotamers (HH, ΔHT, and ΛHT) may be observed when **L** = symmetrical bidentate ligand, whereas four rotamers (HHa, HHb, ΔHT, and ΛHT) are possible when **L** = unsymmetrical bidentate ligand (Figure 8). The symmetry

(35) Bondi, A. *J. Phys. Chem.* **1964**, *68*, 441−451.
(36) Chassot, L.; Muller, E.; Zelewsky, A. V. *Inorg. Chem.* **1984**, *23*, 4249−4253.

Figure 5. In-plane views of the two rings in **bipy**$PtCl_2$ (left) and **L**$PtCl_2$ (right).

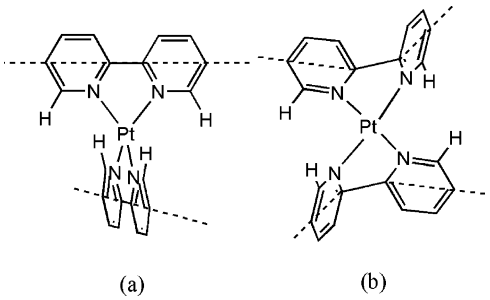

Figure 6. Canting (a) and bowing (b) of the two bipyridyl ligands with respect to each other in [(**bipy**)$_2$Pt]X_2.

of the carrier ligand influences not only the number of conformers but also the number of sets of Guo signals detectable for each [**L**Pt(Guo)$_2$]$^{2+}$ rotamer. For a nonbulky **L**, rotation about the Pt−N7 Guo bond is very fast on the NMR time scale; the rapid equilibration of rotamers in this case leads to one set or two sets of Guo NMR signals for [**L**Pt(Guo)$_2$]$^{2+}$ adducts with symmetrical and unsymmetrical **L**, respectively. Bulky carrier ligands restrict the rotation of Guo about the Pt−N7 bond sufficiently to allow detection of different rotamers by NMR spectroscopy.[21,37−43] Because the Guo H8 signals are downfield, they can be particularly informative for assessing the nature and distribution of rotamers. For an [**L**Pt(Guo)$_2$]$^{2+}$ adduct with an unsymmetrical **L**, the four rotamers should give two and eight H8 signals for rapidly and slowly exchanging conformers, respectively.

For [(**MepyMe$_2$t**)Pt(Guo)$_2$]$^{2+}$, three bound Guo H8 signals were present (Figure 9): two H8 signals of comparable intensity at 8.90 and 8.87 ppm (integrating to a total of one proton) and another larger H8 signal upfield at 8.75 ppm (integrating to a single proton). The observation of three H8 signals (not two for fast or eight for slow isomerization) suggests the occurrence of a complicated equilibration process between rotamers and/or an intermediate exchange rate.

The most likely process accounting for the three signals is rapid rotation of a Guo in one of the coordination positions and slow rotation of the other Guo. This situation would give two pairs of HT and HH conformers that interchange within the pair but not between pairs. In this case, the presence of three H8 signals with one large (the upfield H8) signal requires an overlap of two of the four expected H8 signals. The upfield Guo H8 signal could not be resolved, even at −4.0 °C. However, when the pH was raised to 7.75, four distinct H8 peaks of comparable intensity were observed at 8.88, 8.86, 8.71, and 8.68 ppm (Figure 9). At this pH, the N1H of coordinated Guo is deprotonated, resulting in greater dispersion of H8 signals, but less dispersion for the H1′ signals, which all overlap. However, at pH 4.60, there are two H1′ signals. One H1′ signal (at 6.06 ppm, for one Guo) is one-third as large as the other overlapped H1′ signal (at 6.04 ppm, for three Guo's). Thus, results for both H8 and H1′ signals at both pH's support the presence of four different Guo's in two sets of similarly abundant HT/HH pairs.

Extensive studies in which both the symmetrical carrier ligand and the guanine derivative (**G**) were varied systematically indicate that, for a given adduct, the HT rotamers (in total) are favored over the HH rotamer(s) (in total).[44] Although the reasons for this observation are not fully understood, the most compelling explanations are that base dipole−dipole alignment favors the HT over the HH arrangement of guanines and that clashes between the exocyclic O6 on each guanine in the HH arrangement disfavor the HH rotamer. When **G** is a guanosine 5′-monophosphate, additional complications arise, increasing the abundance of the HH form in some cases, but in general Guo adducts have a particularly low amount of the HH rotamer.[21,41,43] In a previous study of [**L**Pt**G**$_2$]$^{2+}$ adducts with an unsymmetrical **L**, 2-(aminomethyl)piperidine (**pipen**), four H8 signals were observed for each adduct,[45,46] as found here. The results were interpreted as indicating that each pair of H8 signals arose from a rapidly interchanging pair of conformers, ΔHT/HHa and ΛHT/HHb (Figure 8), with the HT form dominating. In

(37) Cramer, R. E.; Dahlstrom, P. L. *Inorg. Chem.* **1985**, *24*, 3420−3424.
(38) Cramer, R. E.; Dahlstrom, P. L. *J. Am. Chem.* Soc. **1979**, *101*, 3679−3681.
(39) Xu, Y.; Natile, G.; Intini, F. P.; Marzilli, L. G. *J. Am. Chem. Soc.* **1990**, *112*, 8177−8179.
(40) Ano, S. O.; Intini, F. P.; Natile, G.; Marzilli, L. G. *Inorg. Chem.* **1999**, *38*, 2989−2999.
(41) Sullivan, S. T.; Ciccarese, A.; Fanizzi, F. P.; Marzilli, L. G. *Inorg. Chem.* **2001**, *40*, 455−462.
(42) Kiser, D.; Intini, F. P.; Xu, Y.; Natile, G.; Marzilli, L. G. *Inorg. Chem.* **1994**, *33*, 4149−4158.
(43) Saad, J. S.; Scarcia, T.; Shinozuka, K.; Natile, G.; Marzilli, L. G. *Inorg. Chem.* **2002**, *41*, 546−557.
(44) Natile, G.; Marzilli, L. G. *Coord. Chem. Rev.* **2006**, *250*, 1315−1331.
(45) Wong, H. C.; Coogan, R.; Intini, F. P.; Natile, G.; Marzilli, L. G. *Inorg. Chem.* **1999**, *38*, 777−787.
(46) Wong, H. C.; Intini, F. P.; Natile, G.; Marzilli, L. G. *Inorg. Chem.* **1999**, *38*, 1006−1014.

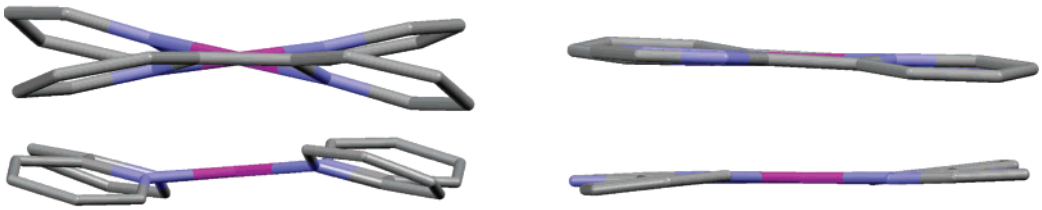

Figure 7. Side view of $[(\mathbf{bipy})_2Pt]X_2$ (left) and $[(\mathbf{pyt})_2Pt]X_2$ (right).

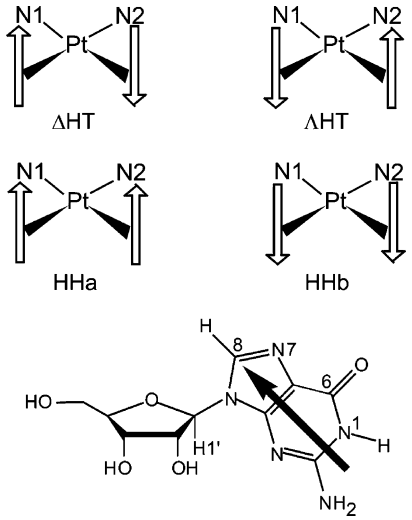

Figure 8. Possible base orientations of two cis guanine bases coordinated to Pt. Each arrow represents a guanine base (bottom). The Pt carrier ligand is to the rear; when it is unsymmetrical (N*1* ≠ N*2*), there are two HH conformers. Rotation of one base about the Pt−N7 bond leads to another conformer, but in each case, the base orientation changes from HT to HH and vice versa. When the carrier ligand has unsymmetrical bulk, it is possible that on the NMR time scale the base next to the bulky side of the carrier ligand does not rotate quickly, whereas the other base rotates rapidly. For example, the ΔHT conformer would interchange rapidly with the HHa conformer if the base next to N*1* rotated slowly while the base next to N*2* rotated readily. In contrast, the ΔHT conformer would form the HHb conformer only slowly.

the **pipen** case, the amino group allows rapid rotation of the cis **G**, whereas the piperidine ring hinders rotation of the cis **G**.[45,46]

The properties of the $[(\mathbf{MepyMe_2t})Pt(Guo)_2]^{2+}$ adduct at pH 7.75 were explored further by using 2D NMR spectroscopy. An additional 1 equiv of Guo was added to ensure that all of the Pt compound was consumed prior to a ROESY experiment, which allows us to probe the exchange processes and the through-space interactions between Guo and the **MepyMe$_2$t** ligand. Neither nuclear Overhauser effect (NOE) nor exchange spectroscopy cross peaks were observed between the H8 signals. An HH conformer would give an H8−H8 NOE cross peak, and even for a rapid HT/HH equilibrium, a cross peak would be found if either HT/HH pair had a significant amount of the HH conformer. The four $[(\mathbf{MepyMe_2t})Pt(Guo)_2]^{2+}$ H8 signals thus reflect mainly the two HT conformers, ΔHT and ΛHT, present in a nearly 1:1 ratio. The H8 NMR signals of the HH conformer were not detectable, indicating a more rapid rate of rotation about the Pt−N7 bond for one Guo in $[(\mathbf{MepyMe_2t})Pt(Guo)_2]^{2+}$, a result more similar to that found for (**pipen**)Pt**G**$_2$ adducts[45,46] than for (**5,5′-Me$_2$bipy**)Pt**G**$_2$ adducts[21] and (**Me$_2$ppz**)Pt**G**$_2$ adducts[41] (**Me$_2$ppz** = *N*,*N*′-dimethylpiperazine).

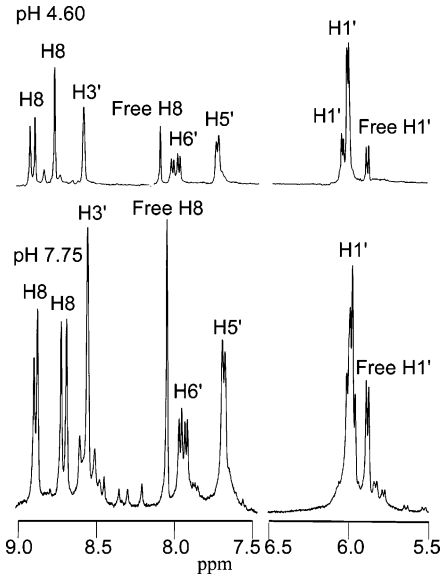

Figure 9. Aromatic and H1′ signals of the ^{1}H NMR spectrum of the $[(\mathbf{MepyMe_2t})Pt(Guo)_2]^{2+}$ adduct in a D_2O/DMSO-d_6 solution at pH 4.60 (top) and pH 7.75 (bottom) at 25 °C. Numbers are taken from the numbering system in Scheme 1 for **L** and are shown in Figure 8 for Guo.

NOE cross peaks in the $[(\mathbf{MepyMe_2t})Pt(Guo)_2]^{2+}$ ROESY spectrum between the Guo H8 singlet at 8.86 ppm and the pyridyl H*6*′ doublet at 7.96 ppm and between the Guo H8 singlet at 8.88 ppm and the pyridyl H*6*′ doublet at 7.94 ppm indicate that the two most downfield H8 signals belong to the Guo bound cis to the pyridyl ring. The more upfield H8 signals, at 8.71 and 8.68 ppm, belong to the Guo bound cis to the triazine ring.

Compared to the signals of $[(\mathbf{MepyMe_2t})Pt(Me_2SO\text{-}d_6)Cl]^+$ in D_2O/DMSO-d_6 at pH 4.60, the H*5*′ (7.76 ppm) and H*3*′ (8.60 ppm) signals of the $[(\mathbf{MepyMe_2t})Pt(Guo)_2]^{2+}$ adduct at pH 4.60 shifted only slightly upfield and downfield, respectively. In contrast, the H*6*′ doublets at 8.04 and 8.00 ppm (integrating to a total of one proton) for this adduct were shifted upfield by ∼1.26 ppm from the H*6*′ signal at 9.28 ppm of $[(\mathbf{MepyMe_2t})Pt(Me_2SO\text{-}d_6)Cl]^+$. The anisotropy of the cis-coordinated guanine base is responsible for these large upfield shifts. These shifts and the H8−H*6*′ NOE cross peaks leave no doubt that the guanine in the adduct is positioned very close to H*6*′. Two considerations [(a) the pyridyl H*6*′ proton is known to hinder the rate of rotation about the Pt−N7 Guo bond[21] and (b) two upfield-shifted H*6*′ signals are resolved for the $[(\mathbf{MepyMe_2t})Pt(Guo)_2]^{2+}$ adduct] leave no doubt that the slowly rotating Guo is cis to the pyridyl ring and that the Guo cis to the triazine ring is in fast rotation. Otherwise, the H*6*′ doublets would probably be time-averaged.

Conclusions

Regardless of the presence of various exocyclic groups, 3-(2′-pyridyl)-1,2,4-triazine ligands are excellent bidentate sp^2 N donors and form both **L**$PtCl_2$ and $[\mathbf{L}_2Pt]^{2+}$ complexes. The juxtaposition of the pyridyl H6′ proton and the triazine lone pair of electrons in $[\mathbf{L}_2Pt]X_2$ allows the formation of a planar structure. Also, this juxtaposition favors the trans arrangement of the bidentate ligands in $[\mathbf{L}_2Pt]X_2$. The ligands prefer to bind via only the N*2* of the triazine ring. No evidence was found for isomers having N*4* coordinated to Pt. Very likely, this result arises from the effect of the group ortho to the bound N. For a given bidentate ligand, the interactions between the juxtaposed groups on the two rings ortho to the bridging C atoms and on the periphery of the bidentate ligand are favorable for 3-(2′-pyridyl)-1,2,4-triazine ligands but unfavorable for **bipy**'s. This favorable factor would be present if the triazine ring binds to metals via either N*2* or N*4*. For N*2* binding, the N*1* lone pair is readily accommodated sterically, but the substituent on C*5* would create steric clashes if metal binding were to occur via N*4*. Thus, the observation that only N*2* binding was detected can be understood. When combined with the X-ray structural results, the H6′ NMR spectral shifts of the complexes containing the **L**'s examined here establish that the structures of virucidal **ptt** compounds containing **ferene** proposed earlier were correct.[13]

The dynamic properties of the [(**MepyMe$_2$t**)Pt$(Guo)_2]^{2+}$ adduct indicate that the lone pair on the nonbonded nitrogen, N*1*, of the triazine ring is not sterically demanding. This lone pair does not strongly impede the rotation of Guo about the Pt−N7 bond, whereas the equivalently placed CH group of the pyridyl ring does impede rotation. This behavior and the structural data all point to a lower overall steric effect of the N*2*-metal-bound triazine ring compared to the metal-bound pyridine ring. Dynamic behavior similar to that of the [(**MepyMe$_2$t**)Pt$(Guo)_2]^{2+}$ adduct has been well documented previously only in the case of **pipen** complexes.[45,46]

Our result that Guo did not add to $[(\mathbf{MepyMe_2t})_2Pt]^{2+}$ suggests the possibility that the virucidal activity of the **L**$PtCl_2$ and $[\mathbf{L}_2Pt]^{2+}$ **ptt** agents arises respectively from covalent and noncovalent (possibly intercalative nucleic acid interactions favored by $[\mathbf{L}_2Pt]^{2+}$ planarity) binding to biomolecular targets. These results suggest that the relatively neglected 3-(2′-pyridyl)-1,2,4-triazine ligands should be examined more widely in coordination chemistry.

Note Added in Proof: A Re complex with the **pyPh$_2$t** ligand was recently characterized crystallographically. Das, S.; Chakravorty, A. *Eur. J. Inorg. Chem.* **2006**, 2285−2291.

Acknowledgment. This work was supported by NIH Grant GM 29222 (to L.G.M.).

Supporting Information Available: Crystallographic data for (**pyMe$_2$t**)$PtCl_2$, (**pyPht**)$PtCl_2$, (**pyPh$_2$t**)$PtCl_2$, and $[(\mathbf{pyPh_2t})_2Pt](BF_4)_2$ in CIF format, ^{1}H NMR spectra and chemical shifts for selected $[\mathbf{L}_2Pt]X_2$ complexes, and a description of reactions of **pyMe$_2$t** with *cis*-$Pt(Me_2SO)_2Cl_2$ studied by ^{1}H NMR spectroscopy. This material is available free of charge via the Internet at http://pubs.acs.org.

IC060605H